

# Homogeneous light stimulation of melanopsin and cones with a Maxwellian view device for the human eye

1<sup>st</sup> Flückiger Patrick  
Instant-lab

Swiss Federal Institute of Technology Lausanne (EPFL) University of Applied Sciences of Western Switzerland (HES-SO)  
Neuchâtel, Switzerland  
patrick.fluckiger@epfl.ch

2<sup>nd</sup> Schmid Jessica

Institute of Industrial Automation  
Yverdon, Switzerland  
jessica.schmid@heig-vd.ch

3<sup>nd</sup> Evéquoz Gilles

Institute of System Engineering  
HES-SO  
Sion, Switzerland  
gilles.evequoz@hevs.ch

4<sup>th</sup> Bressy Pierre

Institute of Industrial Automation  
HES-SO  
Yverdon, Switzerland  
pierre.bressy@heig-vd.ch

5<sup>nd</sup> Geiser Martial

Institute of System Engineering  
HES-SO  
Sion, Switzerland  
ORCID 0000-0002-1017-2872

**Abstract**—We designed and tested a device to stimulate specifically one photoreceptor type, or a combination of some of them, of the human eye by using up to six primaries. The device produces a homogeneous light field over 40° which is projected onto the retina through a Maxwellian view optical system. It avoids the use of an artificial pupil, does not need pupil dilation and retinal illumination can be easily controlled. We successfully tested it with four primaries for melanopsin and S-cone stimulation while maintaining other photoreceptors at a fixed level in photopic regime.

**Index Terms**—vision, silent substitution, ophthalmology device, human eye, Maxwellian view

## I. INTRODUCTION

The human eye can convert light into biological signals through five different photoreceptors. Rods are used for scotopic and mesopic vision, cones S, M and L for mesopic and photopic vision and melanopsin. The latter is optimized for signaling temporal changes in irradiance [2] and contributes to a diverse range of non-visual responses to light such as the circadian rhythm [3], pupillary light response [4], [5] or regulation of rest-activity states and sleep [6], [7].

The signals from these photoreceptors are processed and sometimes combined with each other before being sent to other organs, mainly the brain but also, for example, the pupil. Due to the superposition of the photoreceptor sensitivities (Fig. 1), it is practically impossible to stimulate only a single one. On the other hand, if the light source is sufficiently modulable, it is possible to put several photoreceptors at the same level of excitation and to modulate only one of them (linear system). This technique, called "silent substitution" [8], is used in many research projects, most recently for the study of melanopsin [9]. The signals of these photoreceptors are preprocessed and combined before being brought to the brain.

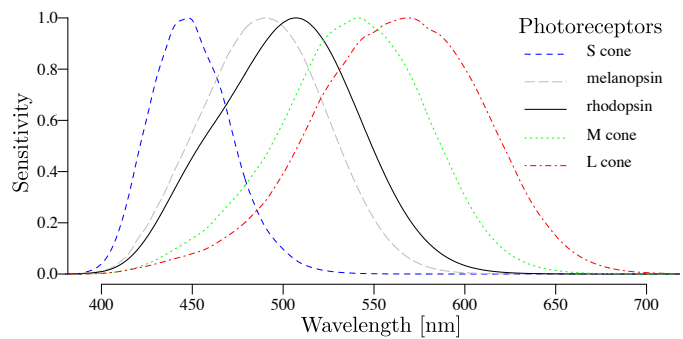


Fig. 1: Sensitivity of the photoreceptors as given by the toolbox of International Commission on Illumination (CIE) [11]

Correct light mixing, homogeneous light fields, large field of view and strict control of the amount of light entering the eye are the difficulties to be overcome in such devices. The latter is usually done with an artificial pupil placed as close as possible to the eye. Besides being uncomfortable, it reduces the field of view in an uncontrolled manner because the position of the eye is not clearly defined. We present, in this paper, a simple but reliable device which easily controls the amount of light without an artificial pupil and with a large controlled field of view. This device allows the pupil measurement of the stimulated eye which is not possible with an artificial pupil.

This device could be used for many applications in vision, in neuro-ophthalmology and in ophthalmology. The presented device is based on a prototype [10] for which the electronics and the software were completely redesigned. This device will be used for experiments in the field of sleep research and in ophthalmology.

## II. MATERIAL AND METHOD

### A. Device

The device consists of an optical instrument with electronics mounted on an ophthalmology table and a computer to control the experiment.

1) *Optics*: The optical system is based on a fundus camera with the front lens  $LS$  of Nextsight (Padova, Italy). It is designed for a field of view of  $40^\circ$  in the eye (Fig. 2). Six LEDs pig-tailed to fibers between  $400\ \mu\text{m}$  and  $800\ \mu\text{m}$  in diameter are connected to an integrating sphere of 5 cm in diameter. The exit hole  $A$  of 4 mm in diameter is imaged by the front lens into the pupil of the eye with a magnification factor of  $\frac{1}{2}$ . In the intermediate image ( $I$ ), an obscuration corresponding to a field of  $10^\circ$  with a fiber end of  $200\ \mu\text{m}$  in diameter in the center. This fiber is connected to a green led so that the central part of the obscuration plays the role of a fixation target. In the tested device, only four LEDs were used: 405 nm, 505 nm, 625 nm from Thorlabs and 598 nm from Seoul Semiconductor. Two monochrome cameras (Imaging Development Systems, Germany, MT9V032C12STM) were used to align the subject at the correct distance, one inline ( $C_2$ ) by using the reflected light on the hot mirror  $M$  and one aiming the eye from below ( $C_1$ ). Only the latter was used to measure the pupil size because the pupil magnification on  $C_2$  is too sensitive to a small axial displacement of the eye. Four NIR LED around the front lens  $FL$  at 920 nm illuminate the pupil.

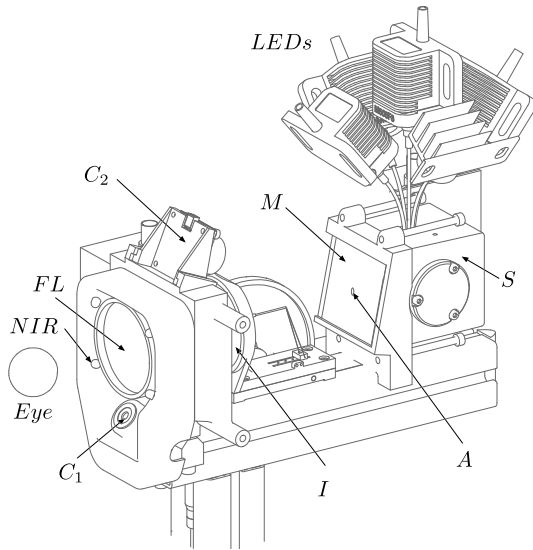


Fig. 2: Drawing of the device with the NIR illumination for the cameras  $C_1$  and  $C_2$ , the front lens  $FL$ , the intermediate image  $I$  mounted on a movable rail to adapt for the dioptry of the *Eye*, the integrating sphere  $S$  with exit hole  $A$ , the primaries  $LEDs$  and the heat mirror  $M$

2) *Electronics*: The LEDs are driven with a microcontroller STM32 based on a processor 32 bits ARM Cortex-M7 from STMicroelectronics. There are two kinds of led drivers:

- For LEDs with an integrated driver modular with a voltage between 0V and 5V, the microcontroller outputs a pulse width modulation (PWM) at 9.6 kHz between 0V and 3.3V which goes through an active low pass filter of the 2nd order with a gain of 1.51 and a cutoff frequency at 400 Hz. The choice of the PWM frequency is a compromise between the resolution of the PWM of the microcontroller and the step resolution of the light intensity. The higher the frequency is, the higher the light intensity resolution will be and the lower the PWM resolution will be.
- For LEDs without an integrated driver, the microcontroller output is a continuous voltage. It is proportionally converted into current, which goes through the LED, by using an operational amplifier circuit and a MOSFET (metal–oxide–semiconductor field-effect transistor). The current is modulated between 0mA (0V) and 660mA (3.3V).

The LEDs are powered with five separated step-downs to keep the power supplies as stable as possible. The electronic part communicates with a computer with a serial COM port using an FTDI chip. The FTDI converts the  $I^2C$  from the microcontroller to a USB port. Both cameras acquired images at 60 frames per second with a resolution of  $752 \times 480$  pixels and  $C_1$  captures in real time of the area of the pupil.

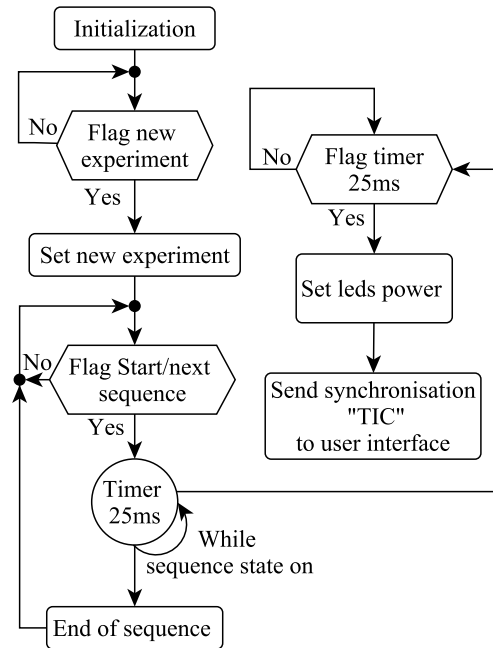


Fig. 3: Firmware flowchart, explaining how the microcontroller synchronises the intensity changing of the LEDs with the image processing realised by the user interface.

3) *Software*: The software consists of three parts:

- Based on the measurement of the LEDs (see Sect. II-B), a code written in R [12] defines the light ratios of the

LEDs for a given experiment and writes the sequences into a csv file.

- The microcontroller software written in C with the real-time operating system, FreeRTOS [15].
- The user interface software written in C++ [13] using Qt [14].

The user interface reads the csv file defining a session of simulations, acquires images from the cameras, processes the images to calculate the size of the pupil and writes the results into files. On the other side, the microcontroller receives the data's experiment from the user interface, drives the LEDs and sends "TICS" (synchronisation messages) via USB to the interface to synchronise the change of light intensity with the image acquisition and processing, as shown in Fig. 3. The typical interval between two acquisitions is 25 ms. The image processing time is the critical part which makes it difficult to reduce the time between two acquisitions. Indeed, the process to get the area of the pupil requires multiple steps. First, the image has to be binarized to make it possible to detect blobs. Then, when the pupil blob is found, the area can be deduced from the number of pixels of the blob and the pixel size. Finally, to get the two axis of the pupil, the blob is modeled by an ellipse with two radii corresponding to the pupil radius. The library OpenCV [16] is used to make the image processing algorithm.

### B. Calibration

The photoreceptors stimulation is described by the vector  $PS = (l, m, s, g)$  in which the elements are the stimulations of respectively the long, medium and short cones and melanopsin. To reach a given  $PS$ , each LED emits with a luminance ratio ranging between 0% and 100% of its maximum. These luminance ratios are described by the vector  $LR$ . The link between photoreceptors stimulation  $PS$  and the LED luminance ratio  $LR$  is assumed to be a linear transformation given by the  $P2C$  matrix where:  $PS = P2C \cdot LR$ . The luminance ratio of each LED is obtained by providing their respective currents (also ranging from 0% to 100%) described by the vector  $I$ . A link between  $LR$  and  $I$ , which we define as calibration, has to be determined. For this step, two methods are presented which will be compared in Sect. III-A.

The first calibration method assumes linearity between  $I$  and  $LR$  and relies on measuring the LED spectra at their maximal intensity in order to create the  $P2C$  matrix. The photoreceptor stimulation  $PS$  for a given set of LED currents  $I$  is then given by  $PS = P2C \cdot I$ . This simple method neglects LED non-linearities and has a high sensitivity to measurement noise (Fig. 4).

The second method modelises the LED luminance with respect to current as quadratic functions which are obtained by regression. For each LED, the current is incremented and the luminance is measured. A quadratic regression is then fitted over each curve. This model assumes that for a given LED only the intensity is non-linear and the proportions in which it stimulates each photoreceptor remain the same.

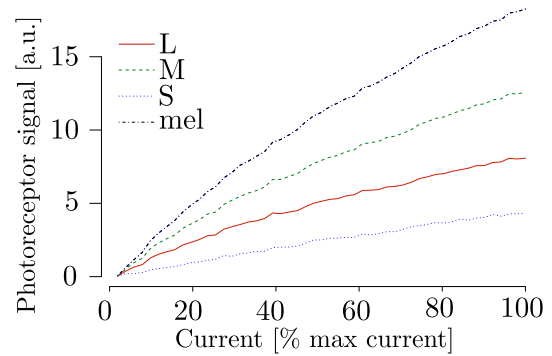


Fig. 4: Photoreceptors stimulations for the green LED as a function of the current driving the LED [% of max current]. Non-linearity is the main issue with this LED.

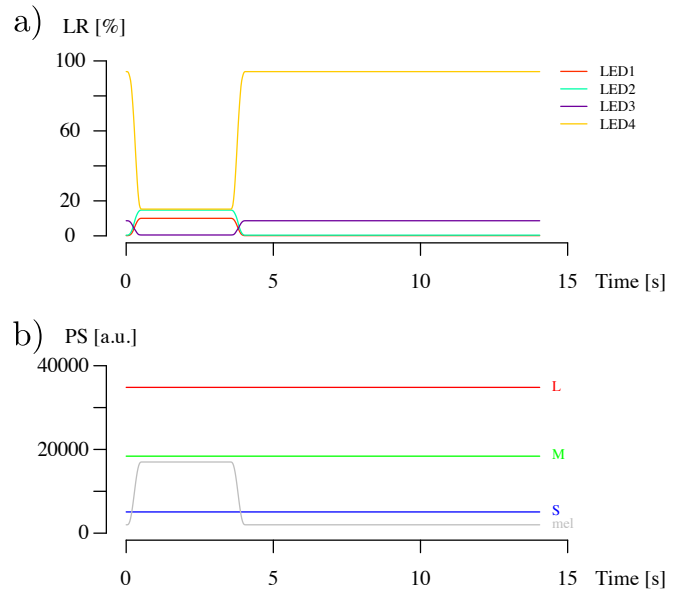


Fig. 5: Example of a melanopsin stimulation: a) light ratio as a function of the time and b) photoreceptor stimulations.

Both methods consider that the peak emission wavelength of each LED are independent of  $I$  and thus do not affect the proportions in which a LED stimulates each photoreceptor.

### C. Set-up of an experiment

The set-up of an experiment starts with the measurements of each LED and its maximum illuminance at the exit pupil of the device. By combining the maximum power spectra of each LED and the photoreceptor sensitivities from CIE [11], we calculate the matrix  $P2C$  and a linearization conversion of the power of the LED. Depending on the proposed stimulation (blue, red, LMS, melanopsin, ...), a contrast mapping (for example for melanopsin in the chromaticity diagram) and a color choice is performed. This allows the time layout of the stimulation (Fig. 5) to be written in csv file, which will be subsequently read and performed by the interface software of the device.

	$K_l$	$K_m$	$K_s$	$K_g$
First method [%]	0.34	5.29	2.25	34.23
Second method [%]	0.24	1.28	0.73	51.73

TABLE I: Percent Michelson contrasts  $K_l, K_m, K_s, K_g$  respectively for l, m, s cones and melanopsin between metamers with a high and low melanopsin stimulation for both methods.

### III. METHOD

#### A. Evaluation of the calibration method

To evaluate whether the second calibration method is indeed more precise than the first, we measured the spectra of high and low melanopsin stimulation metamers generated using both methods. Their respective photoreceptor Michelson contrasts were determined using a provided CIE toolbox which gives each photoreceptor stimulation from a measured spectrum. The objective was to compare the relative variation of cone stimulation between the metamers for both methods (if perfect metamers were obtained, these variations would be zero).

#### B. Comparison with a previous published experiment

Based on the work of Spitschan [1], the goal was to measure the pupillary response for a variety of stimulations. These include stimulation of melanopsin, of S-cones and L+M-cones. The pupillary response was evaluated by measuring the pupil area. On the contrary to Spitschan who used a sinusoidal stimulation, we used pulsed stimulation. For this reason, the phase shift and amplitude changes were extracted from the phase shift and amplitude of the FFT at the stimulation frequencies.

The stimulation patterns consisted in a set of five repeated sequences of 10 rectangular pulses at the following periods: 10s, 5s, 2s and 1s.

The experiments were performed on two male subjects: *A* and *B* (resp. 26 and 62 years old). These were led in a dark room and the subjects were exposed to the lower stimulation level for one minute, in order that the eye got adapted before starting the flickering stimulation.

### IV. RESULTS

#### A. Evaluation of the calibration method

The calculated photoreceptor stimulations of a high and low melanopsin excitation are compared between the first and the second method. Table I shows that Michelson contrast  $K$  for cones is close to zero as expected and that of melanopsine is much higher.

The measured melanopsin contrast of 51.7% obtained with the second method is close to its theoretical value of 50.7% when calculating the currents given to the LEDs.

#### B. Comparison with a previous published experiment

The obtained frequency responses for the three types of excitations are shown in Fig. 7. In comparison, the data of the previous study can be found in the publication of Spitschan et al. [1].

Fig. 6 also shows the average pattern with respect to time for L+M, S and melanopsin stimulations at 0.2 Hz.

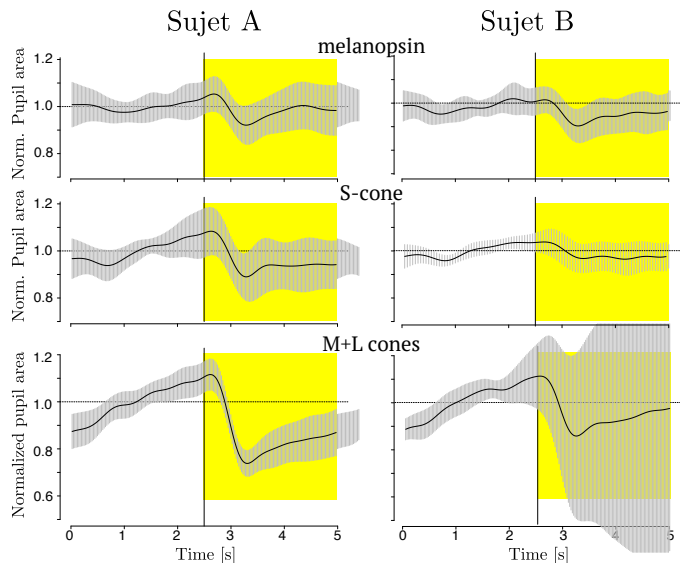


Fig. 6: Relative pupil area for two subjects A (left) and B (right) undergoing flicker stimulation with a period of 5s (0.2Hz) for melanopsin (top), S-cone (middle) and L+M cones (bottom) at resp. 50%, 50% and 35% Michelson contrast.

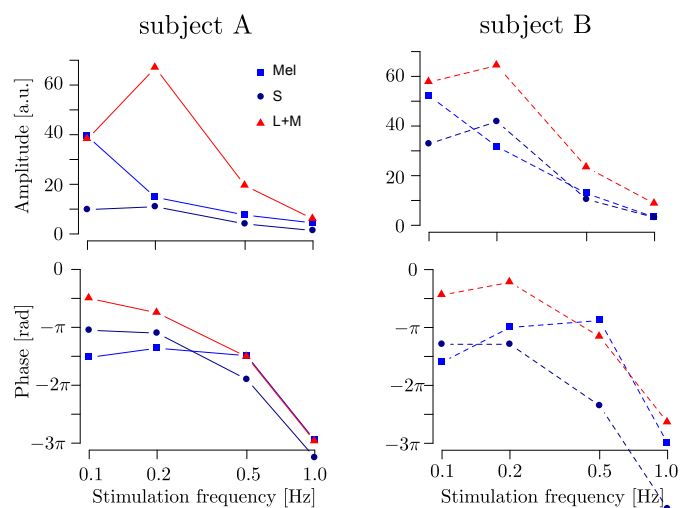


Fig. 7: Amplitude (top) and phase retrieved from the FFT (bottom) of the recordings of four stimulation frequencies done for melanopsin, S-cone and L+M-cones stimulation on two subjects A (left) and B (right).

## V. DISCUSSION

### A. Evaluation of the calibration method

The second calibration method proved to be more precise than the first as the M and S contrasts were significantly reduced and L contrast remained low. Moreover, not only were metamers obtained with sufficient precision, but the obtained melanopsin contrast was also as expected.

After consideration, it can be assumed that the device stimulates the photoreceptors correctly.

### B. Comparison with a previous published experiment

The criteria on which we focus for the comparison between previous and new data are:

- The accumulation of delay in the phase shift.
- The almost constant phase shift between L+M and S stimulations.
- The frequency at which L+M amplitude reaches its maximum is approximately 0.2[Hz].

A prominent resemblance is the constant difference of phase shift between L+M and S stimulations for all experiments, even though this difference is not identical between subjects of the new study and the previous one. Indeed, the initial study showed a difference of  $\pi$  for both subjects, while the current results show differences of approximately 0.4 and 1.1 for subjects *A* resp. *B*. Moreover, in all cases, the delay in the phase shift increases almost linearly with respect to excitation frequency.

Another resemblance among this study's subjects and also with the previous data is the peak of amplitude at approximately 0.2[Hz].

## VI. CONCLUSION

Our device produces homogeneous luminous fields with a view of  $40^\circ$ . The device is also capable of producing metamers with a melanopsin contrast in a controlled manner. Measurements done on two subjects gave very similar results as those published by Spitschan so that we are confident that this device could be used for melanopsin stimulation experiments. Using the device arranged as an ophthalmoscope used in all ophthalmological practices allowed easy and comfortable trials on subjects. Calibration and retinal illuminance measurements are easy, no pupil dilatation is required and eye pupil under stimulation is measured.

## ACKNOWLEDGMENT

This work started with funding from the University of Applied Science of Western Switzerland (96040 / IA-RAD19-02) and was terminated with funding from InnoSuisse (43316.1). Thanks to Manuel Spitschan for his advice during numerous video conferences and Serge Amoos for the construction of the device.

## REFERENCES

- [1] Spitschan, Manuel and Jain, Sandeep and Brainard, David H. and Aguirre, Geoffrey K., "Opponent melanopsin and S-cone signals in the human pupillary light response" vol. 111, no. 43, pp. 15568–15572, 2014.
- [2] T.M. Brown et al., "Melanopsin-based brightness discrimination in mice and humans.," vol. 22, no. 12, pp. 1134–1141, Jun. 2012.
- [3] D.M. Berson et al., "Phototransduction by retinal ganglion cells that set the circadian clock.," vol. 295, no. 5557, pp. 1070–1073, Feb. 2002.
- [4] R.J. Lucas et al., "Characterization of an ocular photopigment capable of driving pupillary constriction in mice.," vol. 4, no. 6, pp. 621–626, Jun. 2001.
- [5] D.S. Joyce et al., "The Effects of Short-Term Light Adaptation on the Human Post-Illumination Pupil Response.," vol. 57, no. 13, pp. 5672–5680, Oct. 2016.
- [6] J.W. Tsai et al., "Melanopsin as a sleep modulator: circadian gating of the direct effects of light on sleep and altered sleep homeostasis in *Opn4(-/-)* mice.," vol. 7, no. 6, p. e1000125, Jun. 2009.
- [7] G. C. Brainard et al., "Human melatonin regulation is not mediated by the three cone photopic visual system.," *J Clin Endocrinol Metab*, vol. 86, no. 1, pp. 433–436, Jan. 2001.
- [8] Spitschan, Manuel and Woelders, Tom, "The Method of Silent Substitution for Examining Melanopsin Contributions to Pupil Control", *Frontiers in Neurology*, 2018
- [9] V. Conus and M. Geiser, "A Review of Silent Substitution Devices for Melanopsin Stimulation in Humans," *Photonics*, vol. 7, no. 4, p. 121, Nov. 2020.
- [10] S. Agrici et al. "Device for silent substitution excitation of melanopsin for human eye," *Ophthalmic Technologies XXIX*, SPIE, vol. 277, pp. 36–7, 2019.
- [11] CIE, "System for Metrology of Optical Radiation for ipRGC-Influenced Responses to Light, CIE S 026 TOOL-BOX", International Commission on Illumination, Vienna, Austria, doi:10.25039/S026.2018.TB, Available online: <http://cie.co.at/news/launch-cie-s-026-toolbox-and-user-guide>
- [12] R Core Team (2019). R: A language and environment for statistical computing. R Foundation for Statistical Computing, Vienna, Austria. ISBN 3-900051-07-0, <http://www.R-project.org/>.
- [13] Programming Language C++14, ISO/IEC. (2014).
- [14] QT 5.15.2 msvc2019.64, <https://www.qt.io/product/development-tools>
- [15] STM32Cube with FreeRTOS, Real-time operating system for microcontrollers, [https://www.st.com/resource/en/user\\_manual/dm00105262-developing-applications-on-stm32cube-with-rtos-stmicroelectronics.pdf](https://www.st.com/resource/en/user_manual/dm00105262-developing-applications-on-stm32cube-with-rtos-stmicroelectronics.pdf)
- [16] OpenCV (Open Source Computer Vision Library), <https://opencv.org/about/>